arXiv:1402.3171v2 [nucl-th] 13 Mar 2014

Three-body model calculations of $N\Delta$ and $\Delta\Delta$ dibaryon resonances

Avraham Gal[a], Humberto Garcilazo[b]

[a] *Racah Institute of Physics, The Hebrew University, 91904 Jerusalem, Israel*
[b] *Escuela Superior de Física y Matemáticas*
Instituto Politécnico Nacional, Edificio 9, 07738 México D.F., Mexico

Abstract

Three-body hadronic models with separable pairwise interactions are formulated and solved to calculate resonance masses and widths of $L = 0$ $N\Delta$ and $\Delta\Delta$ dibaryons using relativistic kinematics. For $N\Delta$, $I(J^P) = 1(2^+)$ and $2(1^+)$ resonances slightly below threshold are found by solving πNN Faddeev equations. For $\Delta\Delta$, several resonances below threshold are found by solving $\pi N\Delta$ Faddeev equations in which the $N\Delta$ interaction is dominated by the $1(2^+)$ and $2(1^+)$ resonating channels. The lowest $\Delta\Delta$ dibaryon resonances found are for $I(J^P) = 0(3^+)$ and $3(0^+)$, the former agreeing well both in mass and in width with the relatively narrow $\mathcal{D}_{03}(2370)$ resonance observed recently by the WASA@COSY Collaboration. Its spin-isospin symmetric partner $\mathcal{D}_{30}$ is predicted with mass around 2.4 GeV and width about 80 MeV.

Keywords:
Faddeev equations, nucleon-nucleon interactions, pion-baryon interactions, dibaryons
PACS: 11.80.Jy, 13.75.Cs, 13.75.Gx, 21.45.-v

1. Dedication

This work is dedicated to the memory of Gerry Brown who has charted and shaped up the frontiers of Nuclear Physics for about half a century. Dibaryons, among many other topical subjects, fascinated Gerry and he has contributed imaginatively to this subject, too. We feel honored to add our modest contribution to this memorial issue of Nuclear Physics A.

2. Introduction

Non-strange s-wave dibaryon resonances $\mathcal{D}_{IS}$ with isospin I and spin S were predicted by Dyson and Xuong [1] in 1964 as early as SU(6) symmetry for baryons, placing the nucleon $N(939)$ and its P_{33} πN resonance $\Delta(1232)$ in the same **56** multiplet, proved successful. These authors chose the **490** lowest-dimension SU(6) multiplet in the $\mathbf{56} \times \mathbf{56}$ direct product containing the SU(3)-flavor $\overline{\mathbf{10}}$ and **27** multiplets in which the deuteron $\mathcal{D}_{01}$ and NN virtual state $\mathcal{D}_{10}$ are classified. This gave four non-strange dibaryon candidates with masses listed in Table 1 in terms of constants A, B. Identifying A with the NN threshold mass 1878 MeV, the value $B \approx 47$ MeV was derived by assigning $\mathcal{D}_{12}$ to the $pp \leftrightarrow \pi^+ d$ coupled-channel resonance behavior noted then at 2160 MeV, near the $N\Delta$ threshold (nominally 2.171 MeV). This led in particular to a predicted mass $M = 2350$ MeV for $\mathcal{D}_{03}$, followed since 1977 by many quark-based model calculations as reviewed by us recently [2].

Table 1: SU(6)-predicted masses of non-strange $L = 0$ dibaryons $\mathcal{D}_{IS}$ with isospin I and spin S, using the Dyson-Xuong mass formula $M = A + B[I(I+1) + S(S+1) - 2]$ [1].

$\mathcal{D}_{IS}$	$\mathcal{D}_{01}$	$\mathcal{D}_{10}$	$\mathcal{D}_{12}$	$\mathcal{D}_{21}$	$\mathcal{D}_{03}$	$\mathcal{D}_{30}$
BB'	NN	NN	$N\Delta$	$N\Delta$	$\Delta\Delta$	$\Delta\Delta$
$\mathrm{SU(3)_f}$	$\overline{\mathbf{10}}$	**27**	**27**	**35**	$\overline{\mathbf{10}}$	**28**
$M(\mathcal{D}_{IS})$	A	A	$A+6B$	$A+6B$	$A+10B$	$A+10B$

The $\mathcal{D}_{12}$ dibaryon conjectured by Dyson and Xuong [1] shows up in the ${}^1D_2$ nucleon-nucleon partial wave above the πNN threshold and it is produced by the coupling between the d-wave NN channel and the s-wave $N\Delta$ channel where Δ is the pion-nucleon P_{33} resonance, i.e. the coupling between the two-body NN channel and the three-body πNN channel. Representative values (in MeV) derived phenomenologically in Refs. [3, 4, 5] for the pole position $W = M - \mathrm{i}\Gamma/2$ of $\mathcal{D}_{12}$ are

$$(M, \Gamma): \quad (2176 \pm 6, 107 \pm 23), \quad (2148, 126), \quad (2144, 110), \qquad (1)$$

respectively, in good agreement with the mass value used in Ref. [1]. Another positive-parity dibaryon, with quantum numbers $IJ = 03$, has been observed at $\sqrt{s} = 2.37$ GeV in a kinematically complete measurement of the pion-production reaction $np \to d\pi^0\pi^0$ [6]. Viewed as the $\Delta\Delta$ dibaryon quasibound state $\mathcal{D}_{03}$ it is deeply bound, by about 90 MeV with respect to the $\Delta\Delta$

threshold. An equally intriguing feature of this dibaryon resonance is its relatively small width $\Gamma(\mathcal{D}_{03}) \approx 70$ MeV, considerably below the phase-space expectation $\Gamma_\Delta \leq \Gamma(\mathcal{D}_{03}) \leq 2\Gamma_\Delta$, with $\Gamma_\Delta \approx 120$ MeV. The binding energy of $\mathcal{D}_{03}$ has been calculated in several works using various one-boson-exchange potential (OBEP) models [7, 8, 9] and a variety of quark-based models for the (real) $\Delta\Delta$ interaction [10, 11, 12, 13, 14, 15, 16, 17, 18, 19] leading to binding energies running from a few MeV up to several hundred MeV. However, no calculation other than the one reported by us recently [20] has so far been able to explain its small width.

In the present paper we extend the hadronic model constructed by us for the $\Delta\Delta$ dibaryon resonance $\mathcal{D}_{03}$ [20] in order to study systematically all the s-wave $N\Delta$ and $\Delta\Delta$ dibaryon candidates. With isospin $\frac{1}{2}$ and spin $\frac{1}{2}$ for nucleons, and isospin $\frac{3}{2}$ and spin $\frac{3}{2}$ for Δ's, the allowed range of isospin I and total angular momentum $J = S$ values consists of $IJ = 12, 21, 11, 22$ for $N\Delta$, and $IJ = 01, 03, 10, 12, 21, 23, 30, 32$ for $\Delta\Delta$ in consequence of the Pauli principle requirement $I + J =$ odd for two identical Δ's.

Considering the Δ as a πN resonance, it is straightforward to replace the ΔN system by a πNN system of three stable particles for which Faddeev equations with separable pairwise potentials may be applied to calculate the mass and width of the various $N\Delta$ resonance candidates enumerated above. This program is followed in Sect. 3. For the $\Delta\Delta$ system, if we wish to keep applying three-body Faddeev equations rather than resorting to the more complicated $\pi N\pi N$ four-body Faddeev-Yakubovsky equations, it is necessary to treat initially one of the πN pairs by a stable Δ within a $\pi N\Delta$ three-body model, recovering its decay-width contribution in the last stage of the dibaryon mass and width calculation. This program is followed in Sect. 4. Finally, in Sect. 5 we summarize our work and present additional discussion.

3. $N\Delta$ dibaryons

The $N\Delta$ system in which N and Δ are in a relative orbital angular momentum state $\lambda = 0$ is a three-body system consisting of a pion and two nucleons, where the πN subsystem is dominated by the P_{33} resonant channel (the Δ resonance) and the NN subsystem is dominated by the $^3S_1$ and $^1S_0$ channels. We work in momentum space using Jacobi vector coordinates $\vec{p}_k, \vec{q}_k$ to denote the relative momentum of pair (i, j) and that of particle k with respect to the center of mass (cm) of pair (i, j), respectively, with (i, j, k)

cyclic permutation of (1,2,3). Thus, labeling the pion as particle 1 and the two nucleons as particles 2 and 3, $\vec{p}_1$ is the NN relative momentum and $\vec{q}_1$ is the pion momentum with respect to the cm of the NN pair.

3.1. Two-body interactions

We use separable pairwise interactions fitted to phase shifts in the dominant channels, as deduced from elastic scattering data. Thus, the πN interaction which is dominated by the P_{33} channel at relevant energies is represented by a rank-one separable potential

$$V_3(p_3, p_3') = \lambda_3 g_3(p_3) g_3(p_3'), \tag{2}$$

so that solving the Lippmann-Schwinger equation with relativistic kinematics one obtains a similar form:

$$t_3(\omega_3; p_3, p_3') = g_3(p_3)\tau_3(\omega_3)g_3(p_3'), \tag{3}$$

with

$$\tau_3^{-1}(\omega_3) = \lambda_3^{-1} - \int_0^\infty p_3^2 dp_3 \frac{[g_3(p_3)]^2}{\omega_3 - E_N(p_3) - E_\pi(p_3) + i\epsilon}, \tag{4}$$

where $E_h(p) = \sqrt{m_h^2 + p^2}$ for hadron h with mass m_h. Here, $\tau_3(\omega_3)$ is the propagator of the Δ isobar in the pion-nucleon cm system, with ω_3 the two-body πN cm energy. In the three-body cm system, with W the total three-body cm energy and q_3 the momentum of the spectator nucleon with respect to the two-body πN isobar, this propagator becomes a function of both W and q_3 and its inverse is given by

$$\mathcal{T}_3^{-1}(W; q_3) = \lambda_3^{-1} - \int_0^\infty p_3^2 dp_3 \frac{[g_3(p_3)]^2}{W - \mathcal{E}_3(p_3, q_3) - E_N(q_3) + i\epsilon}, \tag{5}$$

where $\mathcal{E}_3(p_3, q_3) = \sqrt{[E_\pi(p_3) + E_N(p_3)]^2 + q_3^2}$. For $q_3 = 0$, when the three-body cm system degenerates to the two-body cm system, $\mathcal{T}_3$ reduces to τ_3 with a shifted value of energy: $\mathcal{T}_3(W; q_3 = 0) = \tau_3(W - m_N)$.

We considered two different parametrizations for the form factor g_3. Type I is defined by

$$g_3(p_3) = p_3 \exp(-p_3^2/\beta_3^2) + A_3 p_3^3 \exp(-p_3^2/\alpha_3^2). \tag{6}$$

This form factor falls off exponentially upon $p_3 \to \infty$. Type II is defined by

$$g_3(p_3) = \frac{p_3}{(1 + p_3^2/\beta_3^2)^2} + A_3 \frac{p_3^3}{(1 + p_3^2/\alpha_3^2)^3}, \tag{7}$$

which falls off as p_3^{-3} upon $p_3 \to \infty$. The parameters of these two models were fitted to the πN P_{33} phase shifts from Arndt et al. [21] and are listed in Table 2. The fit of Type I is shown in Fig. 2 of Ref. [22] and the fit of Type II looks essentially identical to that of type I. The table also lists the distance r_0 at which the Fourier transform $\tilde{g}_3(r)$ flips sign, which roughly represents the spatial extension of the P_{33} p-wave form factor as discussed in Ref. [22].

Table 2: Separable-potential parameters of the πN P_{33} form factor $g_3(p)$ (2) fitted to phase shifts [21], and the zero r_0 of the Fourier transform $\tilde{g}_3(r)$ [22], for two types of $g_3(p)$ labeled I (6) and II (7).

type	λ_3 (fm^4)	β_3 (fm^{-1})	α_3 (fm^{-1})	A_3 (fm^2)	r_0 (fm)
I	-0.07587	1.04	2.367	0.23	1.36
II	-0.04177	1.46	4.102	0.11	0.91

For the NN interaction we used rank-two separable potentials consisting of one attractive term and one repulsive term:

$$V_1^\gamma(p_1, p_1') = \sum_{m=1}^{2} \lambda_{1\gamma}^m g_{1\gamma}^m(p_1) g_{1\gamma}^m(p_1'), \tag{8}$$

where $\lambda_{1\gamma}^1$ is negative and $\lambda_{1\gamma}^2$ is positive in both fits of the $^3S_1$ ($\gamma = 1$) and $^1S_0$ ($\gamma = 2$) phase shifts. The resulting t matrix is also separable, as follows:

$$t_1^\gamma(\omega; p_1, p_1') = \sum_{m,n=1}^{2} g_{1\gamma}^m(p_1) \tau_{1\gamma}^{mn}(\omega) g_{1\gamma}^n(p_1'), \tag{9}$$

$$\tau_{1\gamma}^{mn}(\omega) = \frac{G_{1\gamma}^{3-m,3-n}(\omega)}{G_{1\gamma}^{11}(\omega) G_{1\gamma}^{22}(\omega) - G_{1\gamma}^{12}(\omega) G_{1\gamma}^{21}(\omega)}, \tag{10}$$

$$G_{1\gamma}^{mn}(\omega) = \frac{1}{\lambda_{1\gamma}^m} \delta_{mn} - (-)^{m+n} \int_0^\infty p_1^2 dp_1 \frac{g_{1\gamma}^m(p_1) g_{1\gamma}^n(p_1)}{\omega - 2E_N(p_1) + i\epsilon}. \tag{11}$$

Form factors of the Yamaguchi type

$$g_{1\gamma}^m(p_1) = \frac{1}{p_1^2 + (\alpha_{1\gamma}^m)^2} \tag{12}$$

were fitted to the deuteron binding energy and the nucleon-nucleon $^3S_1$ and $^1S_0$ phase shifts. The parameters of these NN potentials are given in Table 3 and the calculated phase shifts are compared in Fig. 1 with those deduced from experiment by Arndt et al. [23].

Table 3: Parameters of the rank-two nucleon-nucleon separable potential in the ${}^3S_1$ and ${}^1S_0$ partial waves fitted to NN phase shifts [23].

channel (γ)	$\lambda^1_{1\gamma}$ (fm^{-2})	$\lambda^2_{1\gamma}$ (fm^{-2})	$\alpha^1_{1\gamma}$ (fm^{-1})	$\alpha^2_{1\gamma}$ (fm^{-1})
${}^3S_1$ ($\gamma = 1$)	-5.6	196.75	1.88	5.38
${}^1S_0$ ($\gamma = 2$)	-6.0	12411	1.90	5.60

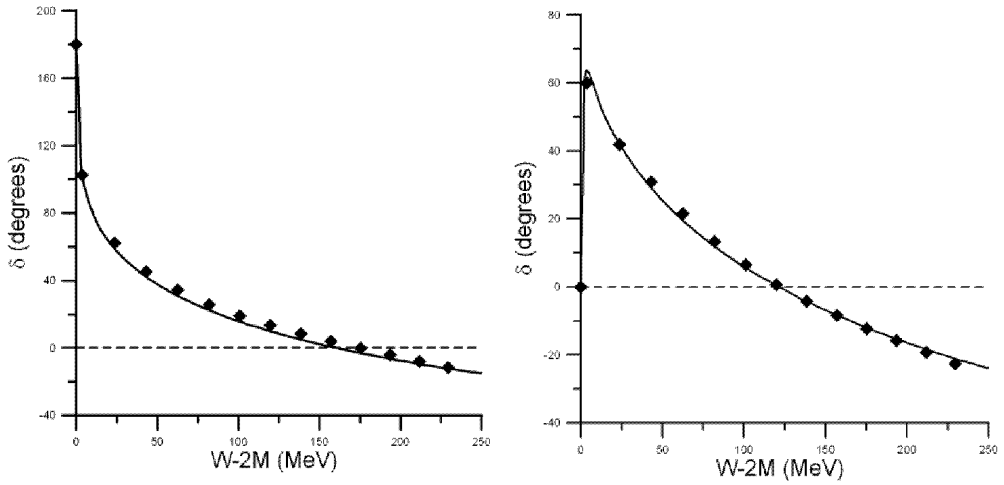

Figure 1: Fits of NN separable potentials to ${}^3S_1$ (left) and ${}^1S_0$ (right) phase shifts [23].

3.2. Faddeev equations of the πNN system

In the case of the πNN system with separable pairwise potentials, since two of the constituents are identical fermions, the Faddeev integral equations reduce to a single integral equation for the $N\Delta$(isobar) T matrix shown diagrammatically in Fig. 2. For a positive-parity πNN state with total isospin I and angular momentum J, this equation is written explicitly as [22]

$$T^{IJ}(W;q_3) = \int_0^\infty dq_3' M^{IJ}(W;q_3,q_3')\mathcal{T}_3(W;q_3')T^{IJ}(W;q_3'), \quad (13)$$

$$M^{IJ}(W;q_3,q_3') = K^{IJ}_{23}(W;q_3,q_3') + 2\sum_{mn\gamma}\int_0^\infty K^{IJ}_{31;m\gamma}(W;q_3,q_1) \times\mathcal{T}^{mn}_{1\gamma}(W;q_1)K^{IJ}_{13;n\gamma}(W;q_1,q_3')dq_1, \quad (14)$$

Figure 2: Diagrammatic representation of the πNN Faddeev equations solved in the present work to calculate $N\Delta$ dibaryon resonance poles.

with a kernel M^{IJ} given in terms of one-particle-exchange amplitudes K_{ij}:

$$K_{23}^{IJ}(W;q_3,q_3') = \frac{1}{2}q_3q_3'\int_{-1}^{1} d\cos\theta\, g_3(p_3)\, g_3(p_3')b_{23}^{IJ} \times\frac{\hat{p}_3\cdot\hat{p}_3'}{W-E_N(q_3)-E_\pi(\vec{q}_3+\vec{q}_3')-E_N(q_3')+i\epsilon}, \quad (15)$$

$$K_{31;m\gamma}^{IJ}(W;q_3,q_1) = \frac{1}{2}q_3q_1\int_{-1}^{1} d\cos\theta\, g_3(p_3)\, g_{1\gamma}^{m}(p_1)b_{31;\gamma}^{IJ} \times\frac{\hat{p}_3\cdot\hat{q}_1}{W-E_N(q_3)-E_N(\vec{q}_1+\vec{q}_3)-E_\pi(q_1)+i\epsilon}, \quad (16)$$

with $K_{13;m\gamma}^{IJ}(W;q_1,q_3) = K_{31;m\gamma}^{IJ}(W;q_3,q_1)$. The momenta $\vec{p}_3,\vec{p}_3'$ in Eq. (15) and $\vec{p}_3,\vec{p}_1$ in Eq. (16) are the pairs relative momenta, given for relativistic kinematics in terms of q_i,q_j and $\cos\theta$ by Eqs. (39)–(43) in Ref. [22]. The factor 2 in Eq. (14) counts the two nucleons, each of which can be exchanged. In Eq. (15), θ is the angle between $\vec{q}_3$ and $\vec{q}_3'$, whereas in Eq. (16) it is the angle between $\vec{q}_1$ and $\vec{q}_3$. Finally, the isospin and angular-momentum recoupling coefficients b_{ij}^{IJ} in Eqs. (15) and (16) are given by [24]

$$b_{ij}^{IJ} = (-)^{I_{ik}+I_j-I}\sqrt{(2I_{ik}+1)(2I_{jk}+1)}\,W(I_jI_kII_i;I_{jk}I_{ik}) \times(-)^{J_{ik}+J_j-J}\sqrt{(2J_{ik}+1)(2J_{jk}+1)}\,W(J_jJ_kJJ_i;J_{jk}J_{ik}), \quad (17)$$

where W's are Racah coefficients in terms of isospins $I_1=1, I_2=I_3=\frac{1}{2}$ with $I_{12}=I_{13}=\frac{3}{2}$ and, independently, angular momenta $J_1=1, J_2=J_3=\frac{1}{2}$ with $J_{12}=J_{13}=\frac{3}{2}$. Note, however, that $I_{23}=0$ is correlated with $J_{23}=1$ ($\gamma=1$) and $I_{23}=1$ with $J_{23}=0$ ($\gamma=2$). The suffix γ in $b_{31;\gamma}^{IJ}$ keeps track of this correlation. These coefficients are listed in Table 4.

Table 4: Recoupling coefficients b_{ij}^{IJ} (17) for πNN Faddeev calculations. The value listed for b_{31}^{11} is independent of the suffix γ, see text.

b_{23}^{12}	b_{31}^{12}	b_{23}^{21}	b_{31}^{21}	b_{23}^{11}	b_{31}^{11}
$-1/3$	$\sqrt{2/3}$	$-1/3$	$\sqrt{2/3}$	$1/9$	$-\sqrt{2/9}$

3.3. Results and Discussion

In order to search for πNN resonances, the integral equation (13) was extended into the complex plane, using the standard procedure $q_i \to q_i \exp(-\mathrm{i}\phi)$ [25] which opens large sections of the unphysical sheet so that one can search for eigenvalues of the form $W = M - \mathrm{i}\frac{\Gamma}{2}$.

Of the four possible $N\Delta$ s-wave states with $IJ = 12$, 21, 11, 22, the last two are found not to resonate. This is easy to understand for the $IJ = 22$ state which cannot benefit from the s-wave NN interactions in the ${}^3S_1$ and ${}^1S_0$ channels. In the case of the $IJ = 11$ state, since $b_{23}^{11} = \frac{1}{9}$ (see Table 4), the K_{23}^{11} amplitude (15) is *repulsive*, and with $(b_{31}^{11})^2 = \frac{2}{9}$ the other component of the kernel M^{11} (14) is too weak to provide sufficient attraction to generate resonances.

The $N\Delta$ states with $IJ = 12$ and 21 are found to resonate. We note that only ${}^3S_1$ enters the calculation of the $IJ = 12$ resonance, while for the 21 resonance calculation only ${}^1S_0$ enters. Furthermore, $b_{23}^{12} = b_{23}^{21}$ and $b_{31}^{12} = b_{31}^{21}$, so that if the ${}^3S_1$ and ${}^1S_0$ interactions were equal, the $IJ = 12$ and $IJ = 21$ resonances would have been degenerate. However, since the ${}^3S_1$ interaction is more attractive than the ${}^1S_0$ interaction, one expects that the $IJ = 12$ resonance lies below the $IJ = 21$ resonance. For the P_{33} interaction model of type I (6), the $IJ = 12$ resonance indeed lies 18 MeV below the $IJ = 21$ resonance, whereas for type II P_{33} interaction model (7), the difference shrinks to merely 10 MeV, as inferred from the calculated masses listed in Table 5. These listed mass values for $IJ = 12$ and $IJ = 21$ are sufficiently close to each other to qualify as approximately degenerate.

We note that the calculated half-widths listed in the table are close to the half-width of the free Δ, as expected naively from a loosely bound $N\Delta$ system. This is also expected within a πNN model provided the πN spatial extension is sufficiently small compared to the NN average distance. If the pion's wavelength were commensurate with the NN average distance, the decay width of the πNN system would have exceeded the free Δ's width, up to ideally twice as much.

Table 5: $N\Delta$ dibaryon S-matrix pole position $W = M - \mathrm{i}\frac{\Gamma}{2}$ (in MeV) for $\mathcal{D}_{12}$ and $\mathcal{D}_{21}$, obtained by solving πNN Faddeev equations for two choices of the πN P_{33} form factor, type I (6) and type II (7) marked by superscripts. The last column lists the results of a nonrelativistic Faddeev calculation by Ueda [26].

$W^{\mathrm{I}}(\mathcal{D}_{12})$	$W^{\mathrm{I}}(\mathcal{D}_{21})$	$W^{\mathrm{II}}(\mathcal{D}_{12})$	$W^{\mathrm{II}}(\mathcal{D}_{21})$	$W^{\mathrm{Ueda}}(\mathcal{D}_{12})$
2147−i60	2165−i64	2159−i70	2169−i69	2116−i61

The mass and width values calculated for the $IJ = 12$ resonance lie comfortably within the range of values exhibited in Eq. (1) for the phenomenologically deduced $\mathcal{D}_{12}$ dibaryon. For this reason we associate the $IJ = 12$ and $IJ = 21$ πNN poles found here with the $\mathcal{D}_{12}$ and $\mathcal{D}_{21}$ dibaryon candidates of Table 1 and Eq. (1). Finally, in the last column of the table we list the result of a πNN Faddeev calculation for $\mathcal{D}_{12}$ by Ueda [26] using nonrelativistic kinematics. Ueda's calculated mass comes about 30 to 40 MeV below the values calculated by us, in rough agreement with our own experience in comparing Faddeev calculations that use relativistic kinematics to similar ones using nonrelativistic kinematics [27].

4. $\Delta\Delta$ dibaryons

Our main interest in this section is in $\Delta\Delta$ dibaryon candidates, particularly the $\mathcal{D}_{03}$ and $\mathcal{D}_{30}$ predicted by Dyson and Xuong [1], see Table 1. As shown in the previous section, describing $N\Delta$ systems in terms of a stable nucleon (N) and a two-body πN resonance (Δ) leads to a well defined πNN three-body model in which $IJ = 12$ and 21 resonances are generated. These were identified by us with the $\mathcal{D}_{12}$ and $\mathcal{D}_{21}$ dibaryons of Table 1 and Eq. (1). This relationship between $N\Delta$ and πNN may be generalized into relationship between a two-body $B\Delta$ system and a three-body πNB system, where the baryon B stands for N, Δ, Y (hyperon) etc. In order to stay within a three-body formulation we need to assume that the baryon B is stable. For $B = N$, this formulation reduces to the one discussed in the previous section for $N\Delta$ dibaryons. For $B = \Delta$, once properly formulated, it relates the $\Delta\Delta$ system to the three-body $\pi N\Delta$ system, suggesting to seek $\Delta\Delta$ dibaryon resonances by solving $\pi N\Delta$ Faddeev equations, with a stable Δ. The decay width of the Δ resonance will have to be considered at the penultimate stage of the calculation. In terms of two-body isobars we have then a coupled-channel

problem

$$B\Delta \leftrightarrow \pi D, \tag{18}$$

where D stands generically for appropriate dibaryon isobars: $\mathcal{D}_{01}$ and $\mathcal{D}_{10}$, which are the NN isobars identified with the deuteron and virtual state respectively, for $B = N$; $\mathcal{D}_{12}$ and $\mathcal{D}_{21}$ for $B = \Delta$.

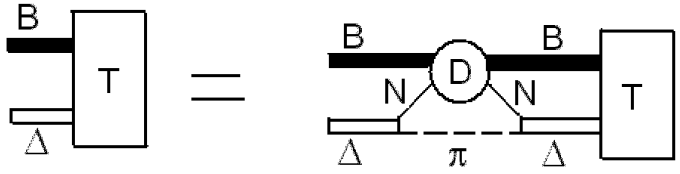

Figure 3: Diagrammatic representation of the πNB Faddeev equations solved to calculate $B\Delta$ dibaryon resonance poles.

Within the set of Faddeev equations for three *stable* particles π, N and B, we label the π meson as particle 1, the nucleon N as particle 2 and the stable baryon B as particle 3, and let these particles interact pairwise through separable potentials. The interaction V_3 between π and N is limited to the P_{33} channel which is dominated by the Δ resonance. Similarly, the interaction V_1 between N and B, for $B = \Delta$, is limited to the $IJ = 12$, 21 channels corresponding to the $\mathcal{D}_{12}$ and $\mathcal{D}_{21}$ dibaryon resonances calculated in the previous section. Finally, the interaction V_2 between the π meson and B is neglected for $B = \Delta$, for lack of known isobar resonances to dominate it. Within this model, the coupled-channel $B\Delta - \pi D$ eigenvalue problem reduces, again, to a single integral equation for the $B\Delta$ T matrix shown diagrammatically in Fig. 3, where starting with a $B\Delta$ configuration the Δ-resonance isobar decays into πN, followed by $NB \to NB$ scattering through the D-isobar with a spectator pion, and ultimately by means of the inverse decay $\pi N \to \Delta$ back into the $B\Delta$ configuration.

Since $\mathcal{D}_{12}$ in the $IJ = 12$ channel appears as a resonance in the NN ${}^1D_2$ partial wave, we will adjust the NB separable potential to that piece of experimental information. In the case of the $IJ = 21$ channel, unfortunately, there is no corresponding experimental information available so that we will have to rely on theoretical arguments based on the similarity between the channels $IJ = 12$ and $IJ = 21$.

4.1. Quantum statistics correlations

The formulation of Faddeev equations for the πNB system requires that B is a stable particle. For $B = \Delta$ we would like to grant Δ a *complex* mass, given by its S-matrix pole position, when appearing as spectator in the πN propagator. By doing so we hope to provide a more realistic estimate of the decay width of $\Delta\Delta$ dibaryons. The width contribution of one of the Δ resonances is fully accounted for by the πN isobar that represents it in the three-body model. Care must be exercised, however, to impose the necessary quantum statistics correlations between this pre-existing $N\pi$ pair and the $N\pi$ pair resulting from the other Δ decay. For $\mathcal{D}_{03}$, for example, assuming s-wave nucleons and p-wave pions implies space-spin symmetry for nucleons as well as for pions. With total I=0, Fermi-Dirac (Bose-Einstein) statistics for nucleons (pions) allows for isospins I_{NN}=$I_{\pi\pi}$=0, forbidding I_{NN}=$I_{\pi\pi}$=1, with weights 2/3 and 1/3, respectively, obtained by recoupling the two P_{33} isospins $I_{N\pi} = \frac{3}{2}$ in the I=0 $\Delta\Delta$ state [20]. In the general case, for given values of I, I_{NN} and $I_{\pi\pi}$, we compute the weight $x_I(I_{NN}, I_{\pi\pi})$ with which $\vec{I}_{NN} + \vec{I}_{\pi\pi} = \vec{I}$ is obtained by recoupling from $\vec{I}_{N\pi} + \vec{I}_{N\pi} = \vec{I}$. This is accomplished using a $9j$ recoupling coefficient,

$$x_I(I_{NN}, I_{\pi\pi}) = (2I_{NN}+1)(2I_{\pi\pi}+1)(2I_{N\pi}+1)^2 \begin{Bmatrix} 1/2 & 1 & I_{N\pi} \\ 1/2 & 1 & I_{N\pi} \\ I_{NN} & I_{\pi\pi} & I \end{Bmatrix}^2 , \quad (19)$$

with a similar expression in spin space for $x_J(S_{NN}, L_{\pi\pi})$. A width-suppression fraction x_{IJ} is defined by summing up over all quantum-statistically allowed products:

$$x_{IJ} = \sum_{I_{NN}, I_{\pi\pi}, S_{NN}, L_{\pi\pi}} x_I(I_{NN}, I_{\pi\pi}) x_J(S_{NN}, L_{\pi\pi}). \quad (20)$$

If the quantum-statistics requirement is relaxed, and summation is extended over all possible couplings, then $x_{IJ} = 1$ by completeness. The values of x_{IJ} according to Eq. (20) are listed in Table 6.

Table 6: Values of width-suppression factors x_{IJ} (20) for $\Delta\Delta$ dibaryons.

IJ	01	10	03	30	12	21	23	32
x_{IJ}	13/27	13/27	2/3	2/3	14/27	14/27	1/3	1/3

4.2. Two-body interactions

The P_{33} πN interaction was already specified in Eqs. (2)-(7), so we need only to construct the NB interactions that generate the $\mathcal{D}_{12}$ and $\mathcal{D}_{21}$ dibaryon resonances. Starting with $\mathcal{D}_{12}$, we wish to construct a separable-potential model that describes the NN $^1D_2$ partial wave below and above the πNN threshold. The simplest choice would be to consider a model that couples the NN and $N\Delta$ two-body channels. However, this model will not generate the inelastic πNN cut at its correct position, since the mass of the Δ is much higher than $m_N + m_\pi$. Therefore we added another s-wave NN' channel, where N' is an auxiliary stable baryon with quantum numbers $I(J^P) = \frac{1}{2}(\frac{3}{2}^+)$ and mass $m_{N'} = m_N + m_\pi$. Note that $J_{N'} = \frac{3}{2}$ is mandatory in order to connect to $J(\mathcal{D}_{12}) = 2$, and $I_{N'} = \frac{1}{2}$ comes natural because the other option $I_{N'} = \frac{3}{2}$ is already taken up by the P_{33} channel for the $\pi - N$ isobar Δ resonance. Note also that N', with $\frac{1}{2}(\frac{3}{2}^+)$, has nothing to do with the P_{13} πN channel. Having introduced the auxiliary N' baryon, we fitted the NN amplitude of Arndt et al. [23] in the $^1D_2$ partial wave using the three-channel separable potential

$$V_1^{mn}(p_1, p_1') = \lambda_1 g_1^m(p_1) g_1^n(p_1'); \quad m, n = 1 - 3, \tag{21}$$

where the three channels are $1 = NN$ (d-wave), $2 = NN'$ and $3 = N\Delta$, both s-wave, with a stable Δ of mass $m_\Delta = 1232$ MeV and quantum numbers $I(J^P) = \frac{3}{2}(\frac{3}{2}^+)$. This coupled-channel system is written generically as NB, where B stands for (N, N', Δ), and its t-matrix is obtained by solving the Lippmann-Schwinger equation with relativistic kinematics,

$$\begin{aligned} t_1^{mn}(\omega_1; p_1, p_1') &= V_1^{mn}(p_1, p_1') + \sum_{r=1}^{3} \int_0^\infty p_1''^2 dp_1'' \, V_1^{mr}(p_1, p_1'') \\ &\quad \times \frac{1}{\omega_1 - E_N(p_1'') - E_r(p_1'') + i\epsilon} t_1^{rn}(\omega_1; p_1'', p_1'), \end{aligned} \tag{22}$$

which in the case of the separable potential (21) has the solution

$$t_1^{mn}(\omega_1; p_1, p_1') = g_1^m(p_1) \tau_1(\omega_1) g_1^n(p_1'), \tag{23}$$

where the propagator of the $\mathcal{D}_{12}$-isobar is expressed through its inverse by

$$\tau_1^{-1}(\omega_1) = \lambda_1^{-1} - \sum_{r=1}^{3} \int_0^\infty p_1^2 dp_1 \frac{[g_1^r(p_1)]^2}{\omega_1 - E_N(p_1) - E_r(p_1) + i\epsilon}, \tag{24}$$

with $m_r = (m_N, m_{N'}, m_\Delta)$ for $r = (1, 2, 3)$. The $r = 2$ NN' channel is responsible for generating the inelastic cut starting at the πNN threshold.

The form factors of the separable potential (21) were taken in the form (which is termed type I)

$$g_1^n(p_1) = \frac{(p_1/o)^\ell}{[1 + p_1^2/(\alpha_1^n)^2]^{1+\ell/2}} \left[1 + A_1^n \frac{(p_1/o)^2}{1 + p_1^2/(\alpha_1^n)^2}\right], \tag{25}$$

where $o = 1$ fm^{-1} ensures that the form factors g_1^n have no units, and with $\ell = 2$ for $n = 1$ and $\ell = 0$ for $n = 2$ and 3. These form factors fall off as p_1^{-2} upon $p_1 \to \infty$. We also considered form factors of a form termed type II:

$$g_1^n(p_1) = \frac{(p_1/o)^\ell}{[1 + p_1^2/(\alpha_1^n)^2]^{3/2+\ell/2}} \left[1 + A_1^n \frac{(p_1/o)^2}{1 + p_1^2/(\alpha_1^n)^2}\right], \tag{26}$$

which fall off as p_1^{-3} upon $p_1 \to \infty$. The inverse-range parameters α_1^n were limited to values $\alpha_1^n \lesssim 3$ fm^{-1} as much as possible to ensure that shorter-range degrees of freedom, for example $\pi N \to \rho N$, need not explicitly be introduced. Good fits to the NN $^1D_2$ scattering parameters satisfying this limitation required that not all A_1^n be zero. Best-fit values of λ_1 and α_1^n in these two models were determined by scanning on selected values of A_1^n and are listed in Table 7. The fitted NN $^1D_2$ phase shifts δ and inelasticities η, defined in terms of the T-matrix by

$$S = 1 + 2\mathrm{i}T = \eta \exp(2\mathrm{i}\delta), \tag{27}$$

are compared in Fig. 4 with values derived from pp scattering experiments [23]. A variance of 0.02 was used for Re T and Im T in these fits. We note that the decrease of the inelasticity η from a value 1 is due to the $r = 2$ NN' subchannel which generates the inelastic cut starting at the πNN threshold, and that no explicit $\mathcal{D}_{12}$ pole term was introduced in the $r = 3$ $N\Delta$ subchannel. Yet, the three-channel system owns a $\mathcal{D}_{12}$ pole, listed in the last column of Table 7.

In the case of the $\mathcal{D}_{21}$ dibaryon there is no experimental information to count on. Since as shown in the previous section $\mathcal{D}_{21}$ and $\mathcal{D}_{12}$ have similar structure and are almost degenerate, it is natural to assume that $\mathcal{D}_{21}$ is generated by the same separable potential model that generates $\mathcal{D}_{12}$. However, with isospin $\frac{1}{2}$ constituents, the NN and NN' channels are unable to couple to total isospin $I = 2$, so alternatively we will replace N' by another auxiliary baryon N'' with $I(J^P) = \frac{3}{2}(\frac{1}{2}^+)$, with the same fit parameters used for $\mathcal{D}_{12}$.

Table 7: Best-fit parameters α_1^n (fm^{-1}) and λ_1 of the three-channel separable potential (21) with type-I (25) and type-II (26) form factors for selected values of A_1^n that provide the lowest χ^2, see Fig. 4, plus pole position W (in MeV) of $\mathcal{D}_{12}$.

g_1	$A_1^1 A_1^2 A_1^3$	χ^2/N	α_1^1	α_1^2	α_1^3	λ_1 (fm^2)	$W(\mathcal{D}_{12})$
I	0 1 $\frac{3}{2}$	1.15	2.04	2.16	2.44	−0.00340	2171−i45
II	0 1 $\frac{3}{2}$	1.12	2.50	2.73	3.16	−0.00287	2176−i49
I	0 1 1	1.10	2.00	2.11	2.96	−0.00313	2172−i58
II	0 1 1	1.05	2.41	2.57	3.74	−0.00296	2179−i61
I	1 1 1	0.78	1.47	2.27	3.24	−0.00214	2177−i63
II	1 1 1	0.70	1.81	3.17	4.44	−0.00132	2182−i74

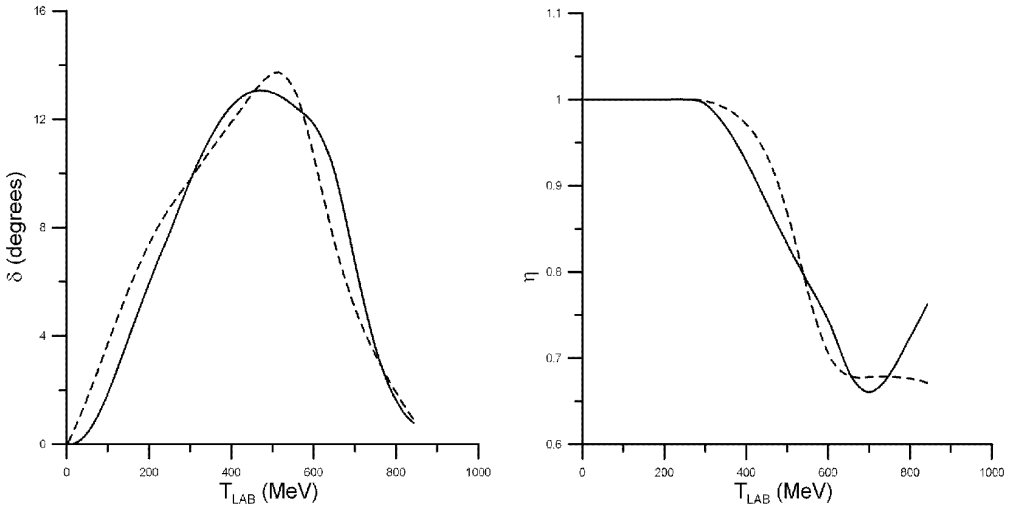

Figure 4: Fits (solid curves) to NN $^1D_2$ scattering parameters (dashed curves) δ (left) and η (right) [23], using the $A_1^j = 1$ ($j = 1, 2, 3$) type-I best-fit parameters from Table 7.

4.3. $B\Delta - \pi D$ coupled-channel πNB Faddeev equations

Using standard three-body techniques [22] the integral equation depicted in Fig. 3 is written explicitly in a vector form, generalizing expression (13) for the πNN system:

$$T_m^{IJ}(W; q_3) = \sum_{n=1}^{3} \int_0^\infty dq_3' M_{mn}^{IJ}(W; q_3, q_3') \mathcal{T}_3^n(W; q_3') T_n^{IJ}(W; q_3'), \qquad (28)$$

where the vectorial indices $m, n = 1, 2, 3$ correspond to the three D-isobar NB channels $(NN, NN', N\Delta)$ or equivalently to the three possible decay channels $B\Delta$=$(N\Delta, N'\Delta, \Delta\Delta)$, and the kernels M^{IJ}_{mn} are given by

$$M^{IJ}_{mn}(W; q_3, q'_3) = 2\sum_{d=1}^{2}\int_0^\infty dq_1 K^{IJ}_{31;md}(W; q_3, q_1)\mathcal{T}_{1;d}(W; q_1)K^{IJ}_{13;nd}(W; q_1, q'_3), \tag{29}$$

where $d = 1, 2$ correspond to the πNN isobars D with $IJ = 12$ and $IJ = 21$. The reason for a factor 2 on the r.h.s. of Eq. (29) is that in the decay of the isobar D, $D \to NB$, the nucleon N can originate from each one of the constituents of D, similarly to the way a factor 2 was justified on the r.h.s. of Eq. (14). The amplitudes $K^{IJ}_{31;nd}(W; q_3, q_1)$ are structured similarly to those specified for the πNN system by Eq. (16):

$$\begin{aligned} K^{IJ}_{31;nd}(W; q_3, q_1) &= K^{IJ}_{13;nd}(W; q_1, q_3) = \frac{1}{2}q_3 q_1 \int_{-1}^{1} d\cos\theta\, g_3(p_3)\, g^n_1(p_1) b^{IJ}_{31;nd} \\ &\times \frac{\hat{p}_3 \cdot \hat{q}_1}{W - E_\pi(q_1) - E_N(\vec{q}_1 + \vec{q}_3) - E_n(q_3) + i\epsilon}, \end{aligned} \tag{30}$$

where $b^{IJ}_{31;nd} = b^{IJ}_{31}$, as given by Eq. (17), with $I_1 = J_1 = 1$, $I_2 = J_2 = \frac{1}{2}$ and $(I_3, J_3) = (\frac{1}{2}, \frac{1}{2}), (\frac{1}{2}, \frac{3}{2}), (\frac{3}{2}, \frac{3}{2})$ for $n = (1, 2, 3)$, respectively, $I_{23} = 1, J_{23} = 2$ for $d = 1$ ($D = \mathcal{D}_{12}$) and $I_{23} = 2, J_{23} = 1$ for $d = 2$ ($D = \mathcal{D}_{21}$). In the latter case only $n = 3$ is effective, since the channels $n = 1, 2$ do not couple to $\mathcal{D}_{21}$. Finally, $I_{12} = J_{12} = \frac{3}{2}$ remains as was for πN.

The propagators of the Δ and D isobars are $\mathcal{T}^n_3(W; q_3)$ and $\mathcal{T}_{1;d}(W; q_1)$, respectively. The expression for $\mathcal{T}^n_3(W; q_3)$, for example, is given in the three-body cm frame by

$$[\mathcal{T}^n_3(W; q_3)]^{-1} = \lambda_3^{-1} - \int_0^\infty p_3^2 dp_3 \frac{[g_3(p_3)]^2}{W - \mathcal{E}_3(p_3, q_3) - E_n(q_3) + i\epsilon}, \tag{31}$$

slightly generalizing the expression (5) for πNN, and similarly for $\mathcal{T}_{1;d}(W; q_1)$. Finally, in the propagator (31) for $n = 3$, the mass of the baryon $B = \Delta$ which up to this point has been assumed to be real is modified to include its width by using the Δ pole position [21], in MeV:

$$m_B = 1232 \quad \to \quad W_\Delta = 1211 - \mathrm{i}x_{IJ}49.5, \tag{32}$$

where the width-suppression factors x_{IJ} are given in Table 6.

4.4. Results and Discussion

The integral equations (28) were solved for the $\Delta\Delta$ dibaryon candidates $\mathcal{D}_{IJ}$, with (i) $IJ = 01, 03, 23$ proceeding exclusively through $D = \mathcal{D}_{12}$ in the πD intermediate state in Fig. 3, (ii) $IJ = 10, 30, 32$ proceeding exclusively through $D = \mathcal{D}_{21}$, and (iii) $IJ = 12, 21$ that proceed through both choices of D. We start by listing results in Table 8 for $\mathcal{D}_{03}$ because of its apparent relevance to the resonance observed recently in the WASA@COSY $pn \to d\pi\pi$ measurements [6]. Partial results were given in Ref. [20].

Table 8: $\mathcal{D}_{03}$ pole position (in MeV) found by solving Eqs. (28) for the three best-fit baryon-baryon interactions labeled by their values of A_1^1, A_1^2, A_1^3, in decreasing order of χ^2, using combinations of form factors $(g_3^{\rm k}, g_1^{\rm k'})$ with k,k' each running on types I and II. The half-width values in parentheses disregard quantum-statistics correlations, i.e. $x_{03} = 1$.

A_1^1, A_1^2, A_1^3	$g_3^{\rm I}\ g_1^{\rm I}$	$g_3^{\rm I}\ g_1^{\rm II}$	$g_3^{\rm II}\ g_1^{\rm I}$	$g_3^{\rm II}\ g_1^{\rm II}$
0,1,$\frac{3}{2}$	2392−i52	2386−i47	2380−i45	2373−i41
0,1,1	2384−i44	2374−i38	2356−i30	2344−i26
1,1,1	2383−i41(47)	2386−i38(44)	2343−i24(31)	2337−i21(28)

The $\mathcal{D}_{03}$ pole positions listed in Table 8 result from calculations that use all four combinations of form factors g_3 and g_1 within each of the three lowest χ^2 fits of V_1 to the ${}^1D_2$ NN scattering parameters marked by their values of the parameters A_1^j $(j = 1, 2, 3)$ from Table 7. The calculated pole positions are sensitive primarily to the choice of πN form factor g_3 from Table 2; the smaller its spatial extension r_0, the lower the calculated mass values are. Admitting values of r_0 appreciably below 0.9 fm, the smaller of the two values chosen here, calls for the introduction of explicit vector-meson and/or quark-gluon degrees of freedom which are outside the scope of the present model. The dependence of the calculated pole positions on the chosen baryon-baryon form factor g_1 of Eqs. (25) and (26) is weaker. For a given choice of g_1, the calculated mass values display sensitivity primarily through the fitted values of the inverse-range parameters α_1^n listed in Table 7, particularly α_1^3. Whereas values of $\alpha_1^3 \lesssim 2.5$ fm^{-1} were found impossible to get, going beyond $\alpha_1^3 \sim 3$ fm^{-1} was considered undesirable, again requiring the introduction of explicit short-range degrees of freedom. For these reasons, the discussion below is limited to results obtained using type I form factor g_1, displaying only the sensitivity to the πN form factor g_3. As for width values $-2{\rm Im}W$, the calculated widths display little sensitivity to these form factors and the

widths are determined primarily by the phase space available for decay. The listed half-widths values were calculated using the width-suppression fraction $x_{03} = \frac{2}{3}$ from Table 6. For comparison we added in parentheses for the lowest χ^2 best fit, last line in the table, the half-width calculated disregarding quantum-statistics correlations, i.e. $x_{03} = 1$. The masses are insensitive to the value of x_{03} used in the calculations. We conclude this discussion of the calculated $\mathcal{D}_{03}$ results by noting that the average over the four results shown in the table for the best fit potential (last line) comes very close to the reported mass $M = 2.37$ GeV and width $\Gamma \approx 70$ MeV of the $\mathcal{D}_{03}$ resonance [6].

Table 9: $\mathcal{D}_{03}$ and $\mathcal{D}_{30}$ pole positions (in MeV) found by solving Eqs. (28) with πN form factor $g_3^{\rm k}$ of types k=I,II. N' denotes the best-fit $NN - NN' - N\Delta$ coupled channel interaction V_1 (last line in Table 8 for $\mathcal{D}_{03}$). N'' stands for replacing $N'(I = \frac{1}{2}, J = \frac{3}{2})$ by $N''(I = \frac{3}{2}, J = \frac{1}{2})$ in the $\mathcal{D}_{30}$ calculation, retaining form factors.

$\mathcal{D}_{IJ}$	$g_3^{\rm I}\ N'$	$g_3^{\rm I}\ N''$	$g_3^{\rm II}\ N'$	$g_3^{\rm II}\ N''$
$\mathcal{D}_{03}$	2383−i41(47)	2383−i41(47)	2343−i24(31)	2343−i24(31)
$\mathcal{D}_{30}$	2411−i41(49)	2391−i39(46)	2370−i22(30)	2350−i22(29)

We proceed now to discuss the exotic $\Delta\Delta$ dibaryon candidate $\mathcal{D}_{30}$, noticing that since in Eq. (30) $b^{03}_{31;31} = b^{30}_{31;32}$ the states $IJ = 03$ and $IJ = 30$ become degenerate in the limit of equal $D = \mathcal{D}_{12}$ and $D = \mathcal{D}_{21}$ isobar propagators. Since $D = \mathcal{D}_{12}$ was found to lie lower than $D = \mathcal{D}_{21}$, we expect also $\mathcal{D}_{03}$ to lie lower than $\mathcal{D}_{30}$. The results of our Faddeev calculations, presented in Table 9, indeed confirm this expectation, placing $\mathcal{D}_{30}$ 28 MeV above $\mathcal{D}_{03}$ for the standard calculation marked N' in the table, and only 8 MeV apart for the calculation in which N' was replaced by N'' (with $I(J^P) = \frac{3}{2}(\frac{1}{2}^+)$ and same fit parameters as used for $\mathcal{D}_{12}$). Such approximate degeneracy was noticed in old OBEP work [7] and in several of the quark-based works [10, 13, 15, 16, 19], and it has been discussed recently in Ref. [28]. In our case it is just a consequence of the approximate $I \leftrightarrow J$ underlying symmetry of our model.

The $\mathcal{D}_{03}$ and $\mathcal{D}_{30}$ are not the only $\Delta\Delta$ dibaryon candidates found as resonances in our Faddeev calculations. In Table 10 we list all the $\mathcal{D}_{IJ}$ resonance poles found using the best-fit V_1 for two choices of the πN form factor g_3. Averaged results are also listed. The table suggests that in addition to the $(\mathcal{D}_{03}, \mathcal{D}_{30})$ doublet, the lowest of all $\Delta\Delta$ dibaryon doublets, two additional $I \leftrightarrow J$ doublets are found several tens of MeV higher in energy and are twice

Table 10: $\mathcal{D}_{IJ}$ pole positions (in MeV) found by solving Eqs. (28) for the best-fit baryon-baryon interaction V_1 with type I g_1 form factors (25) and $A_1^j = 1, j = 1, 2, 3$, using width-suppression fractions x_{IJ} from Table 6 and type I,II g_3 πN form factors, with averaged results denoted W in the last line. Note: $\mathcal{D}_{23}$ is numerically unstable.

g_3	$\mathcal{D}_{03}$	$\mathcal{D}_{30}$	$\mathcal{D}^*_{12}$	$\mathcal{D}^*_{21}$	$\mathcal{D}_{23}$	$\mathcal{D}_{32}$
I	2383−i41	2411−i41	2431−i76	2449−i94	2431−i72	2444−i89
II	2343−i24	2370−i22	2428−i67	2436−i72	2429−i72	2439−i66
W	2363−i33	2391−i32	2430−i72	2443−i83	2430−i72	2442−i78

or more as broad: $(\mathcal{D}^*_{12}, \mathcal{D}^*_{21})$, where the asterisk distinguishes these excited $IJ = 12$ and 21 resonances from the lower $(\mathcal{D}_{12}, \mathcal{D}_{21})$ $N\Delta$ dibaryon resonances of Sect. 3, and the $(\mathcal{D}_{23}, \mathcal{D}_{32})$ doublet of resonances. To understand this hierarchy we recall that by Eq. (30) the kernel M^{IJ} (29) is roughly proportional to the squares of the recoupling coefficients $b^{IJ}_{31;nd}$. For $\mathcal{D}_{03}$ and $\mathcal{D}_{30}$ the squares of the only nonvanishing coefficients $b^{03}_{31;31}$ and $b^{30}_{31;32}$, respectively, assume the maximal value 1. For the other two doublets, several nonvanishing coefficients contribute with average square about 0.5, so that the effective interactions in these systems are weaker than for $\mathcal{D}_{03}$ and $\mathcal{D}_{30}$. It is interesting to note that for the nonresonant dibaryon candidates $\mathcal{D}^*_{01}$ and $\mathcal{D}^*_{10}$ the squares of their only nonvanishing coefficients $b^{01}_{31;31}$ and $b^{10}_{31;32}$, respectively, are 0.125 each, exceedingly small to form resonances.

In order to understand the mechanism for the relatively small widths of $\mathcal{D}_{03}$ and $\mathcal{D}_{30}$, recall the formulation of the three-body πNB model and its $B\Delta - \pi D$ coupled-channel description around Eq. (18), where D corresponds to a three-channel $NB \equiv (NN, NN', N\Delta)$ isobar. The decay of $\mathcal{D}_{03}$ and $\mathcal{D}_{30}$ through the upper $B\Delta \equiv (N\Delta, N'\Delta, \Delta\Delta)$ channel can proceed only via the $\Delta\Delta$ subchannel. In particular, the strong decay expected from the $N'\Delta$ subchannel is forbidden and the resulting effective decay width is reduced to $\approx$(0.3–0.5)Γ_Δ in terms of the free-space Δ decay width $\Gamma_\Delta \approx 120$ MeV. Similar suppression should have occurred for the decay width of $\mathcal{D}_{32}$, but its higher mass provides larger phase space for decay, also elastically to the πD channel. Finally, the $\mathcal{D}^*_{12}$, $\mathcal{D}^*_{21}$ and $\mathcal{D}_{23}$ dibaryon resonances are allowed to decay through all of the $B\Delta$ subchannels and their decay width is not suppressed with respect to Γ_Δ.

5. Summary and Outlook

A unified hadronic approach to the calculation of non-strange dibaryon candidates was presented in this work. The building blocks of the model here applied are nucleons, Δ's and pions, the latter playing a special role. Apart from generating long-range pion-exchange interactions, as in the first diagram on the r.h.s. of the LS equation Fig. 2, the pion forms a Δ resonance by scattering off a nucleon, thereby linking the two baryons of the model. A πNN three-body model was formulated in terms of Faddeev equations to explore $N\Delta$ dibaryons. Separable interactions were fitted to scattering phase shifts in the dominant NN s-wave channels and the πN P_{33} channel. With this input, the πNN Faddeev equations were solved using relativistic kinematics. Resonance poles in the $I(J^P) = 1(2^+), 2(1^+)$ $N\Delta$ channels were found nominally below threshold and were attributed to the $N\Delta$ dibaryon candidates $\mathcal{D}_{12}, \mathcal{D}_{21}$ predicted by Dyson and Xuong [1]. The calculated $I(J^P) = 1(2^+)$ resonance mass and width agree closely with those extracted phenomenologically from NN and πd scattering and reaction data [3, 4, 5]. The existence of the "exotic" $I(J^P) = 2(1^+)$ resonance, in contrast, lacks experimental support or phenomenological evidence because with isospin $I = 2$ it is decoupled from NN scattering data. Of course, given the proximity of these nearly degenerate $N\Delta$ resonances to the $N\Delta$ threshold, and given that their widths are similar to that of a free Δ, it is not an easy task to distinguish them from $N\Delta$ threshold effects.

To study $\Delta\Delta$ dibaryons we formulated a πNB three-body model with pairwise separable interactions in the dominant πN P_{33} channel, as above, and in the NB dibaryon $I(J^P) = 1(2^+), 2(1^+)$ resonating channels. The $I(J^P) = 1(2^+)$ interaction was constrained by the NN $^1D_2$ scattering data without explicitly assuming it to resonate. Special care was taken to ensure that the inverse-range parameters α_1^n of the NB interaction satisfy the constraint $\alpha_1^n \lesssim 3$ fm^{-1} to be consistent with the exclusion of explicit vector mesons and shorter-range degrees of freedom from our long-range physics model. The $I(J^P) = 1(2^+)$ interaction was also employed in the $2(1^+)$ channel in most of the reported calculations. With these input two-body interactions, the πNB Faddeev equations were solved, allowing the Δ constituent of the model to acquire decay width compatible with the requirements of quantum statistics with respect to the pion and nucleon constituents of the model. Several $\mathcal{D}_{IJ}$ dibaryon resonances were found below the $\Delta\Delta$ threshold, notably the $(\mathcal{D}_{03}, \mathcal{D}_{30})$ doublet, with $\mathcal{D}_{03}$ the lowest dibaryon at complex

energy value 2363−i33 MeV, where the theoretical uncertainty of its mass and width values is estimated by ±20 MeV, in good agreement with the resonance observed by WASA@COSY in double-pion production $pn \to d\pi\pi$ reactions [6].

It is remarkable that our long-range physics model calculations reproduce the two nonstrange dibaryons established experimentally and phenomenologically so far, the $N\Delta$ dibaryon $\mathcal{D}_{12}$ [3, 4, 5] and the $\Delta\Delta$ dibaryon $\mathcal{D}_{03}$ reported by the WASA@COSY Collaboration [6]. Among the other dibaryon candidates predicted to resonate in our model calculations, the broad $\mathcal{D}^*_{12}(2430)$ ($\Gamma \approx$140 MeV) deserves attention. It would be useful to place constraints on the appearance of this dibaryon candidate in partial-wave analyses of the $NN\ ^1D_2$ wave. The other predicted dibaryons, a relatively narrow $\mathcal{D}_{30}(2390)$ ($\Gamma \approx$65 MeV) and a doublet of broad resonances $(\mathcal{D}_{23}, \mathcal{D}_{32})$ at 2440 MeV ($\Gamma \approx$160–170 MeV) are all "exotic" in the sense that their high value of isospin forbids them to couple to NN partial waves. Among these "exotic" dibaryon candidates, $\mathcal{D}_{30}(2390)$ is particularly interesting. It was highlighted recently by Bashkanov, Brodsky and Clement [28] who focused attention to the special but unspecified role played by six-quark hidden-color configurations in forming the $(\mathcal{D}_{03}, \mathcal{D}_{30})$ dibaryon resonances. However, the recent quark-based calculations by Huang, Ping and Wang [19] conclude that such configurations enhance binding by merely 15±5 MeV, which is within the theoretical uncertainty claimed in our hadronic-basis calculations.

Acknowledgments

The research of A.G. is supported partially by the HadronPhysics3 networks SPHERE and LEANNIS of the European FP7 initiative. H.G. is supported in part by COFAA-IPN (México).

References

[1] F.J. Dyson, N.-H. Xuong, Phys. Rev. Lett. **13** (1964) 815.

[2] A. Gal, H. Garcilazo, PoS (in press) arXiv:1401.3165.

[3] I.I. Strakovsky, A.V. Kravtsov, M.G. Ryskin, Yad. Fiz. **40** (1984) 429 [Sov. J. Nucl. Phys. **40** (1984) 273]; see also A.V. Kravtsov, M.G. Ryskin, I.I. Strakovsky, J. Phys. G: Nucl. Part. Phys. **9** (1983) L187.

[4] R.A. Arndt, J.S. Hyslop III, L.D. Roper, Phys. Rev. D **35** (1987) 128 and references cited therein.

[5] N. Hoshizaki, Phys. Rev. C **45** (1992) R1424, Prog. Theor. Phys. **89** (1993) 563 and references cited therein.

[6] P. Adlarson, et al. (WASA-at-COSY Collaboration), Phys. Rev. Lett. **106** (2011) 242302; M. Bashkanov, et al. (CELSIUS/WASA Collaboration), Phys. Rev. Lett. **102** (2009) 052301.

[7] T. Kamae, T. Fujita, Phys. Rev. Lett. **38** (1977) 471.

[8] T. Ueda, Phys. Lett. B **79** (1978) 487.

[9] H. Sato, K. Saito, Phys. Rev. Lett. **50** (1983) 648.

[10] M. Oka, K. Yazaki, Phys. Lett. B **90** (1980) 41.

[11] P.J. Mulders, A.T. Aerts, J.J. de Swart, Phys. Rev. D **21** (1980) 2653, and earlier works cited therein.

[12] P.J. Mulders, A.W. Thomas, J. Phys. G: Nucl. Part. Phys. **9** (1983) 1159.

[13] K. Maltman, Nucl. Phys. A **438** (1985) 669; **501** (1989) 843.

[14] T. Goldman, K. Maltman, G.J. Stephenson Jr., K.E. Schmidt, F. Wang, Phys. Rev. C **39** (1989) 1889.

[15] A. Valcarce, H. Garcilazo, R.D. Mota, F. Fernández, J. Phys. G: Nucl. Part. Phys. **27** (2001) L1.

[16] R.D. Mota, A. Valcarce, F. Fernández, D.R. Entem, H. Garcilazo, Phys. Rev. C **65** (2002) 034006.

[17] J. Ping, H. Pang, F. Wang, T. Goldman, Phys. Rev. C **65** (2002) 044003.

[18] J.L. Ping, H.X. Huang, H.R. Pang, F. Wang, C.W. Wong, Phys. Rev. C **79** (2009) 024001.

[19] H. Huang, J. Ping, F. Wang, Phys. Rev. C **89** (2014) 034001.

[20] A. Gal, H. Garcilazo, Phys. Rev. Lett. **111** (2013) 172301.

[21] R.A. Arndt, W.J. Briscoe, I.I. Strakovsky, R.L. Workman, Phys. Rev. C **74** (2006) 045205.

[22] A. Gal, H. Garcilazo, Nucl. Phys. A **864** (2011) 153.

[23] R.A. Arndt, W.J. Briscoe, I.I. Strakovsky, R.L. Workman, Phys. Rev. C **76** (2007) 025209.

[24] T. Fernández-Caramés, A. Valcarce, H. Garcilazo, P. González, Phys. Rev. C **73** (2006) 034004; H. Garcilazo, A. Valcarce, T. Fernández-Caramés, Phys. Rev. C **76** (2007) 034001.

[25] B.C. Pearce, I.R. Afnan, Phys. Rev. C **30** (1984) 2022.

[26] T. Ueda, Phys. Lett. B **119** (1982) 281.

[27] H. Garcilazo, A. Gal, Nucl. Phys. A **897** (2013) 167.

[28] M. Bashkanov, S.J. Brodsky, H. Clement, Phys. Lett. B **727** (2013) 438.